ISBN: 978-3-95450-184-7 doi:10.18429/JACoW-IPAC2018-TUPAL047

STRAIN MEASUREMENT IN THE RECENT SNS MERCURY TARGET WITH GAS INJECTION*

Yun Liu†, Willem Blokland, Cary Long, Sydney Murray III, Bernie Riemer, Robert Sangrey, Mark Wendel, Drew Winder
Spallation Neutron Source, Oak Ridge National Laboratory, Oak Ridge, TN 37831, USA

Abstract

High-radiation-tolerant fiber-optic strain sensors were recently developed to measure the transient proton-beam-induced strain profiles on the mercury target vessel at the Spallation Neutron Source (SNS). Here we report the strain measurement results and radiation-resistance performance on the latest SNS mercury target vessel equipped with helium gas injection. The results have demonstrated the efficacy of gas injection to reduce the cyclic stress on the target module.

INTRODUCTION

The Spallation Neutron Source (SNS) target module is a replaceable stainless-steel vessel through which the mercury is circulated [1]. During the neutron production process, the target module is subjected to short (~700 ns) but intense (up to 23.3 kJ) pulses of protons with an energy of approximately 1 GeV, 60 times per second. These pulses create pressure waves in the mercury which cause stress cycles on the vessel and lead to the development of fatigue cracks. The sudden pressurization induced by the beam, followed by relaxation within the vessel, also leads to cavitation of the liquid mercury, which causes erosion of the target module walls. Fatigue and cavitation erosion damage have led to leaks and limited the lifetimes and power levels of operating targets.

Among other physical parameters, strain is probably most directly relevant to the fatigue life of the target vessel. Therefore, measurement of strains on the target vessel is important to understand the dynamic response of the target to the proton pulse, improve theoretical modelling of target structure, and provides a direct evidence for target damage mitigation methods such as small bubble gas injection [2]. Since 2015, SNS has established the capability to measure the strains in the target by installing fiber-optic sensors in the interstitial space between the mercury vessel and the outer water-cooled shroud. However, high radiation tolerance and high measurement bandwidth imposed major challenges on the commercial fiber-optic sensors.

In this paper, we report the strain measurement performance using the SNS customized fiber-optic strain sensors which have demonstrated an order-of-magnitude higher radiation-tolerance and bandwidth than conventional fiber-optic strain gauges. The sensors have been applied in the recent SNS jet-flow target that was equipped with gas injector hardware for the first time. The strain measurement results have demonstrated the efficacy of gas injection to reduce the cyclic stress on the target module across the location and proton power levels, and through continuous beam operation at 1.2 MW.

* ORNL is managed by UT-Battelle, LLC, under contract DE-AC05-00OR22725 for the U.S. Department of Energy. This research was supported by the DOE Office of Science, Basic Energy Science, Scientific User Facilities. This work has also been supported by U.S. DOE grant DE-FG02-13ER41967.
† liuy2@ornl.gov

SENSOR INSTRUMENTATION

Fig. 1 shows a schematic of the fiber-optic strain sensor developed at SNS. The sensor head consists of a low-finesse Fabry-Perot interferometer (FPI) formed by cleaved end surfaces of two pieces of fibers assembled inside a glass capillary tube. The inset box in Fig. 1 shows a microscopic image of the sensor head. The glass tube has an outer diameter of 209 μm and an inner diameter of 127 μm. A fluorine-doped single-mode fiber from Fujikura (RRSMFB) has been chosen as it demonstrated high radiation tolerance in the light transmission around the wavelength of 1300 nm [3]. The default gap between the two fiber end surfaces is approximately 65 μm and the sensor length is around 7 mm. Each sensor has a 2.5 m long lead fiber with a polyimide coating and the outer diameter of the coating is 250 μm so that it can fit in the interstitial space between the vessel and outer water-cooled shroud.

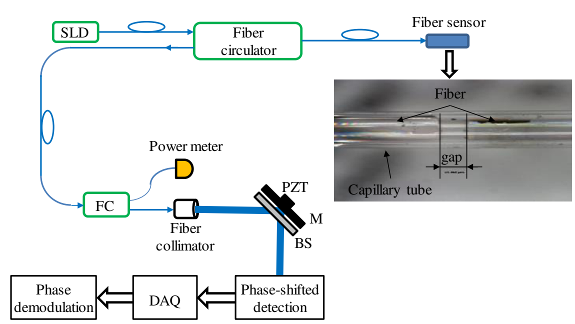

Figure 1: Schematic of fiber-optic strain sensor. SLD: superluminiscent laser diode, PD: photo-detector, FC: fiber coupler, M: mirror, BS: 50/50 beam splitter, PZT: piezoelectric transducer actuator, DAQ: data acquisition unit. Inset box: microscopic image of sensor head.

In the FPI-based fiber-optic sensors, the measurement of physical quantities is performed through an interrogation setup that demodulates the interferometric phase containing the optical path difference (OPD) variations in the sensor head. To minimize the influence due to light source instabilities and power fluctuations from sensing environment, a low-coherence interferometry technique has been employed in the signal detection of the current sensor. A

ISBN: 978-3-95450-184-7 doi:10.18429/JACoW-IPAC2018-TUPAL047

fiber coupled superluminescent laser diode (SLD) is used as a broadband light source. Since the laser coherence length (~ 30 μm) is shorter compared to the default OPD of the sensor head, the reflecting light is coupled into a free-space local receiving interferometer (LRI) for the demodulation of the interferometric phase. The LRI is comprised of two pieces of reflectors forming a Fizeau interferometer. A novel phase demodulation scheme has been implemented which enables effective measurement with high adaptability to variations of the nominal sensor gap caused by ambient temperature and epoxy hardening due to radiation [4].

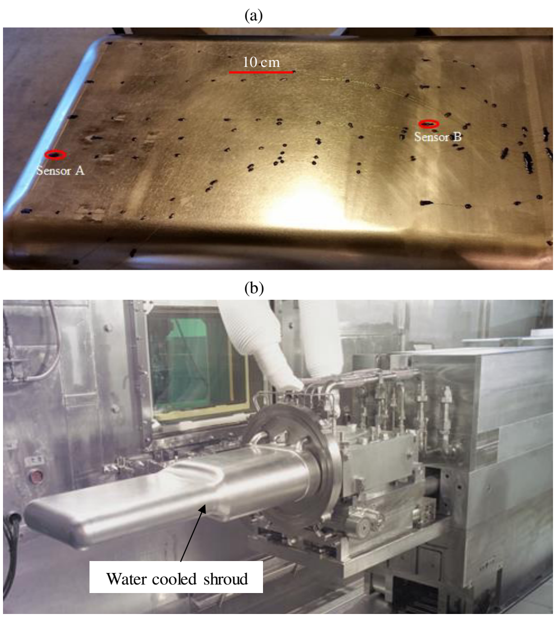

Figure 2: (a) Sensors mounted on the mercury target vessel. Strain measurement results from sensors A and B will be described. (b) Target module (mirrored image) mounted on target carriage in the target service bay. The target vessel is covered by water cooled shroud during operation.

The developed sensors have been applied to strain measurement since 2016. Both measurement bandwidth and radiation tolerance of the sensors have demonstrated an order of magnitude higher than their commercial counterparts [5]. Fig. 2 shows a picture of the sensors mounted on the target vessel T18 (the 18th target used in SNS operation since 2006). The sensor and multiple spots of the lead fiber are mounted to the mercury vessel using a Stycast 2850T epoxy cured with Catalyst 11. The radiation dose (or the absorbed dose) at the sensor and along the fiber cable is calculated based on the energy deposition from all particles including neutrons, protons, and photons on the target vessel. For sensors A and B indicated in Fig. 2(a), the estimated radiation dose rates at the sensor head are 15.9 MGy/MWHr and 1.63 MGy/MWHr, respectively, where the MWHr (or 3.6 GJ) represents the proton beam energy on the target. The water-cooled shroud is mounted after the installation of the sensors. The fiber sensors are connected to the signal processing electronics (located in the target manipulator's gallery) through relay fiber cables. The final connection between the fiber sensors and signal processors is conducted by remote handling after the installation of the target module to the carriage.

STRAIN MEASUREMENTS ON THE TARGET WITH GAS INJECTION

The target T18 was the first target module to be equipped with gas injector hardware at SNS [6]. The fiber-optic strain sensors were used to assess the effects of gas injection to reduce the beam-pulse-induced mercury vessel strains. The initial testing involved pulse-on-demand. The test pulses were varied in pulsed proton flux to represent equivalent power levels at 60 Hz for beam powers of 100 kW – 1.4 MW. Tests without gas injection were performed first. After the tests without gas injection, the gas injection was turned on and strain measurements were conducted for the same pulse proton flux values so that the effects of gas injection could be assessed.

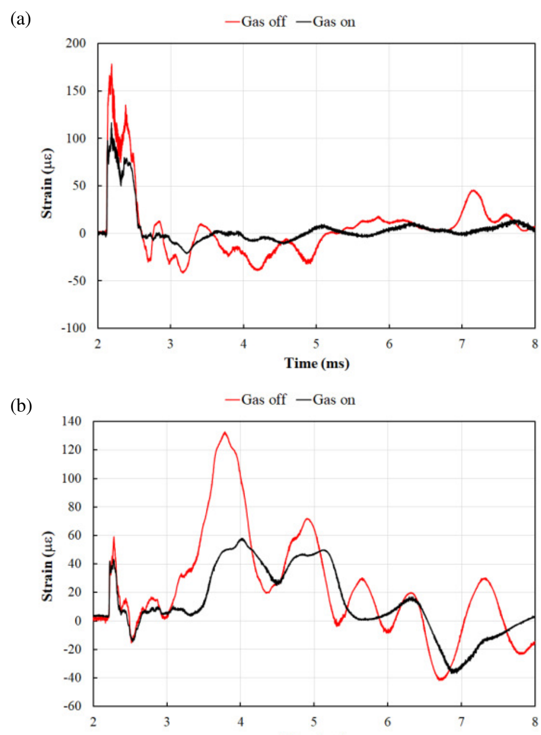

Figure 3: Strain waveforms measured with sensor A (a) and sensor B (b) at gas injection off and on. The proton beam power is 1.2 MW (equivalent) in both cases.

Along with other type of sensors, six single-mode fiber-optic strain sensors have been successfully installed on the current target. Four sensors were mounted near the front of the target and the other two in the back (~ 0.5 m from the front). Fig. 3 shows examples of the measured strain waveforms from sensor A (a) and sensor B (b). In each case, we show strain waveforms of a 1.2 MW proton pulse measured with and without the gas injection. The mechanism for the difference between the strain waveforms measured

ISBN: 978-3-95450-184-7 doi:10.18429/JACoW-IPAC2018-TUPAL047

in the front and back of the target vessel has been discussed in our previous paper [5]. A clear reduction of the strain magnitude due to gas injection has been verified. The strain magnitude reduction percentages were calculated to be about 37% for (a) and 48% for (b). The amount of gas injection is 0.4 standard liter per minute (SLPM) which is about 0.035% of the mercury flow by volume.

The SNS target was switched to the neutron production mode after the initial test. The proton beam power was ramped up to 850 kW in the first week and was then increased to 1.2 MW in the second week. The same proton power was maintained until the end of the operation cycle. While the front sensors were lost in the first week, the strain sensors mounted in the back lasted to the end of the operation cycle. Fig. 4 shows the measured strain magnitude from sensor B from Nov. 7 to Dec. 21, 2017. The proton beam power has been 1.2 MW during the entire period. Compared to the strain magnitude measured without gas injection, the strain magnitude reduction of 50% was observed over almost the entire period.

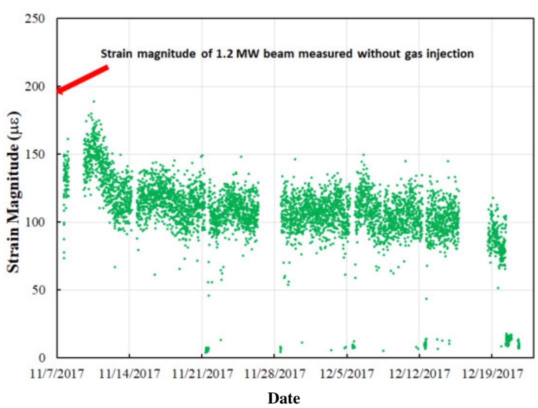

Figure 4: Strain magnitudes of 1.2 MW neutron production beam measured from sensors B on SNS target T18 with gas injection. The reference level indicates the strain magnitude of the 1.2 MW beam measured without gas injection.

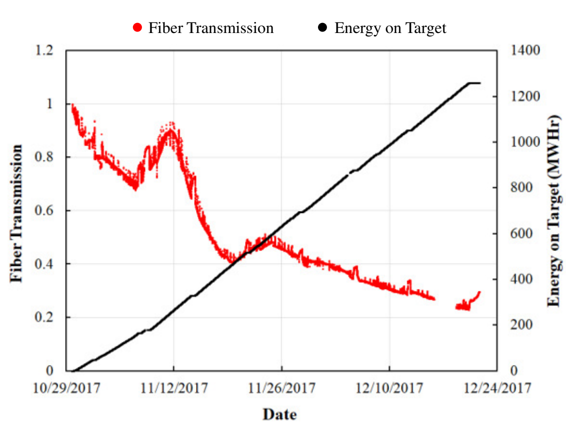

Figure 5: Normalized fiber transmission of sensor B and proton beam energy delivered on the SNS target T18.

To characterize the radiation tolerance of the sensor, we also measured the radiation-induced absorption (RIA) of the fiber during the operation cycle of the target. Fig. 5 shows the measured fiber transmission (normalized to th initial value taken right after the first proton pulse was delivered on the target). The proton beam energy on the target is also plotted in the figure and the radiation dose on the sensor can be calculated from the beam energy. The sensor survived through the entire cycle of the target with an accumulated proton beam energy of 1260 MWHr. The corresponding radiation dose is estimated to be ~ 2×10^9 Gy. The non-uniform variation of the fiber transmission curve is probably due to the slow sensor gap expansion caused by high radiation around the sensor head.

CONCLUSION

Radiation-resistant fiber-optic strain sensors have been developed at SNS to measure the strain in the mercury target. The sensor demonstrated unprecedented radiation tolerance and high bandwidth. The strain measurement studies using the developed fiber-optic sensors has successfully verified the effect of injecting helium gas into the mercury target material.

REFERENCES

[1] R. Haines, T. J. McManamy, T. A. Gabriel, R. E. Battle, K. K. Chipley, J. A. Crabtree, L. L. Jacobs, D. C. Lousteau, M. J. Rennich, and B. W. Riemer, "Spallation neutron source target station design, development, and commissioning," *Nucl. Instrum. Methods Phys. Res. A*, Vol. 764, pp. 94-115, 2014.

[2] B. W. Riemer, M. W. Wendel, D. K. Felde, R. L. Sangrey, A. Abdou, D. L. West, T. J. Shea, S. Hasegawa, H. Kogawa, T. Naoe, C. H. Farny, A. L. Kaminsky, "Small gas bubble experiment for mitigation of cavitation damage and pressure waves in short-pulse mercury spallation targets," *J. Nucl. Mater.*, Vol. 450, pp. 192-203, 2014.

[3] K. Aikawa, K. Izoe, N. Shamoto, M. Kudoh, and T. Tsumanuma, "Raidation-resistant single-mode optical fibers," *Fujikura Technical Review,* pp. 9-13, 2008.

[4] Y. Liu, R. Strum, D. Stiles, C. Long, A. Rakhman, W. Blokland, D. Winder, B. Riemer, M. Wendel, "Digital phase demodulation for low-coherence interferometry-based fiber-optic sensors," *Opt. Commun.*, Vol. 411, pp. 27-32, 2018.

[5] Y. Liu, W. Blokland, C. Long, B. Riemer, M. Wendel, and D. Winder, "Strain measurement in the spallation target using high-radiaiton-tolerant fiber sensors," *IEEE Sensors J.*, Vol. 18, pp. 3645-3653, 2018.

[6] W. Blokland, Y. Liu, M. Wendel, and D. Winder, "Measurements of the effects of gas injection into SNS target T18," *SNS Technical Report*, 106010101-TR0043, 2018.